PICAST 2 – AAC 6
MELBOURNE 20-23 MARCH 1995

New Techniques for Force and Pressure Measurement in Hypervelocity Impulse Facilities

J.M. Simmons, D.J. Mee, S.L. Tuttle, W.J. Daniel, S.C. Overton and A.L. Smith
Department of Mechanical Engineering
The University of Queensland
Brisbane, Australia

Summary A new balance is described for the measurement of aerodynamic forces and moments on models in hypervelocity impulse facilities. Through interpretation of the stress waves propagating in the models, measurements are possible in free-piston shock tunnels and expansion tubes for which test times range from about 100 μs to 1 ms. New measurements in hypervelocity flow in the T4 free-piston shock tunnel at The University of Queensland are compared with theoretical predictions to demonstrate the effectiveness of the balance. They include drag on a 5° semi-angle cone at zero incidence, thrust produced by a scramjet nozzle and lift, drag and pitching moment on a waverider and a 15° semi-angle cone at incidence. Measurements of thrust produced by a fully integrated, scramjet-powered model vehicle are also presented. Extension of the technique to the use of bar gauges for measurement of pressure is reported.

1 INTRODUCTION

The term 'hypervelocity' refers to hypersonic flows (Mach number above about 5) with velocities that are high enough (above about 4 km/s in air) for high temperature molecular phenomena to occur. Hypervelocity impulse facilities, such as shock tunnels and expansion tubes, are needed to generate the flows associated with the external aerodynamics of space planes at near orbital velocities and the internal aerodynamics of scramjet propulsion systems. The free-piston driver technique, developed by Stalker (1) and illustrated in Fig. 1, enables velocities of 7 to 8 km/s to be reached, with enthalpies up to 40 MJ/kg. Test times are only 1 to 3 ms, thereby posing challenges for measurement techniques.

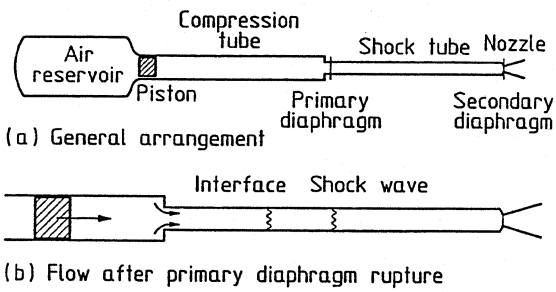

Fig. 1 Operation of free-piston shock tunnel.

In addition to their short test times, free-piston shock tunnels have another complication. Through the creation of a stagnant, high energy reservoir of test gas, dissociation can occur and can be transmitted as a contaminant into the free-stream flow in the test section. This problem is avoided in expansion tubes (Miller (2)) but the unsteady wave processes used to generate high energy flow further restrict the useful test time to as low as 100 μs.

Development of hypervelocity facilities at The University of Queensland has been paralleled by development of new measurement techniques (Simmons (3)). They include a time-of-flight mass spectrometer for species measurement (Skinner (4)), skin friction gauges (Kelly et. al. (5)) and pressure, heat transfer and force transducers. In this paper the authors review their work on force and pressure measurement and present new results from tests of cones, wavericers and scramjets in hypervelocity flow.

2 FORCE MEASUREMENT

2.1 Principle of the Stress Wave Force Balance

Conventional force measuring techniques cannot be used in test flows of only 1 ms duration. Acceleration compensation has enabled them to work in flows as short as 10 ms, but no conventional technique exists for flows of the order of 1 ms. Sanderson and Simmons (6) developed a new technique for measuring drag in hypersonic impulse facilities with test times of 1 ms or less. The balance, referred to here as the 'stress wave force balance', involves attaching the test model to a long, elastic sting and suspending the arrangement such that there is no restriction to movement in the direction of the drag force (Fig. 2). The sudden application of a drag force on the model, which occurs with the arrival of flow in the test section, causes stress waves to propagate and reflect within the model and the sting. A strain gauge mounted on the sting, near the interface between the model and the sting, is used to monitor the strains caused by the stress wave

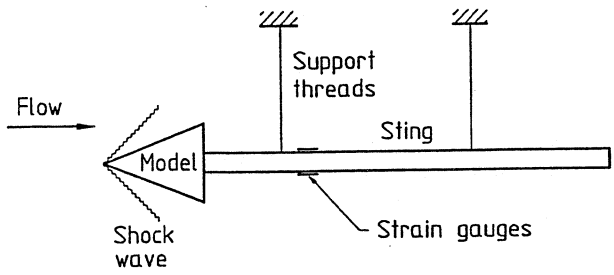

Fig. 2 Schematic of new drag balance.

activity. Such an arrangement can be modelled as a linear system with the input being the time-history of the drag force on the model, $u(t)$, and the output being the strain measured in the sting, $y(t)$. An impulse response, $g(t)$, describes the relationship between this input and output. This system can be described by the convolution integral,

$$y(t)=\int_0^t g(t-\lambda)u(\lambda)d\lambda \qquad (1)$$

In experiments the unknown drag on the model is determined from the measured output strain signal and the impulse response, which is obtained either experimentally or by finite element modelling. Thus, the problem is an inverse one and the drag is found using a numerical deconvolution procedure. The sensitivity of the impulse response to the assumed distribution of loading has been studied by Simmons et al. (7).

2.2 Drag on Cones at Zero Incidence

In the original prototype balance of Sanderson and Simmons (6) a 200 mm long, 15° semi-angle cone was used as the test model. This relatively short cone ensured many reflections of waves within the model during the test time. The authors report that there was no discernible change in the impulse response for the model/sting configuration when the load on the model was changed from a point load at the tip to a uniform pressure over the surface of the cone. The restriction on model size has now been relaxed. The tests on a longer model that are reported here were conducted in order to gauge the robustness of the principle of the stress wave force balance.

The model considered here is a 5° semi-angle cone which is 425 mm in length, more than twice as long as the model used for the prototype balance of Sanderson and Simmons. The solid aluminium cone is attached to a 2 m long circular brass tube (the sting) of 31.8 mm outside diameter and 1.6 mm wall thickness. In the experiments the strain was measured on the sting with strain gauges located 310 mm from the cone/sting interface. The length of the model is such that it takes 170 μs for disturbances to propagate from the cone tip, reflect from the junction between the model and the sting and return to the tip. This is short when compared with a typical test time of 1 ms in The University of Queensland's T4 free-piston shock tunnel.

The experimental technique used to determine the impulse response is to suspend the model/sting arrangement from a fine wire attached to the tip of the model and to cut the wire. This provides a rapid removal of a load from the tip of the model and the model and sting fall freely. The magnitude of the load removed is the weight of the model and sting. In this case the downstream end of the sting is unsupported and stress waves reflect there from a free end.

The experiments performed in the T4 shock tunnel cover a range of nozzle supply enthalpies from approximately 3 MJ/kg to 13 MJ/kg at a nominal Mach number of 5. Nitrogen was used as the test gas to avoid dissociation effects that are possible with air at high enthalpies. Fig. 3 shows a comparison of a typical deconvolved measured drag time-history compared with a theoretical prediction using the cone flow theory of Taylor and Maccoll (8), a skin friction approximation and a base pressure approximation. The temporal variation is based on the time-history of the measured Pitot pressure in the test section of the tunnel. The skin friction is assessed using a reference temperature method and Sutherland's viscosity law. An entirely laminar boundary layer is assumed. Based on this model, the skin friction component of drag is between 12% and 20% of the net drag on the cone. The deconvolution process amplifies the noise, so the results have been filtered using an 8-pole Butterworth low-pass filter with a cut-off frequency of 2 kHz.

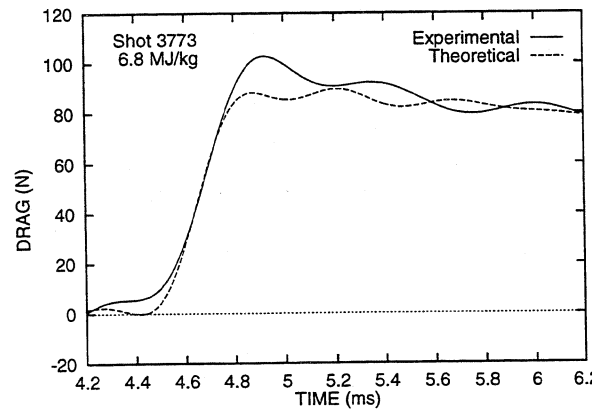

Fig. 3 Comparison of measured and theoretical drag on a 5° cone; test conditions of 6.8 MJ/kg supply enthalpy, 11.5 kPa static pressure, 780 K static temperature, 3400 km/s flow speed and Mach 6.1.

2.3 Thrust from Scramjets

The stress wave force balance has also been used with a two-dimensional thrust nozzle on a scramjet. The loading on the model is not axisymmetric, as in the case of a cone at zero incidence, and the internal flow presents some design difficulties. A two-sting system has been used to accommodate the internal flow in the nozzle and achieve some symmetry. This can be seen in Fig. 4. The nozzle is 300 mm long, the angle of the ramp walls is 11° and the area ratio is 4.76. The situation is complicated by the fact that with the small ramp angle and the internal pressure on the nozzle walls, loading is predominantly transverse. Yet it is

the axial thrust which is to be measured through detection of the tensile waves propagating in the stings. The stings need to be stiffened against bending so it was decided to twist them through 90° just aft of the nozzle. Finite element analysis showed that this does not significantly alter the propagation of the axial stress waves in the sting, but the rigidity of the system is greatly increased.

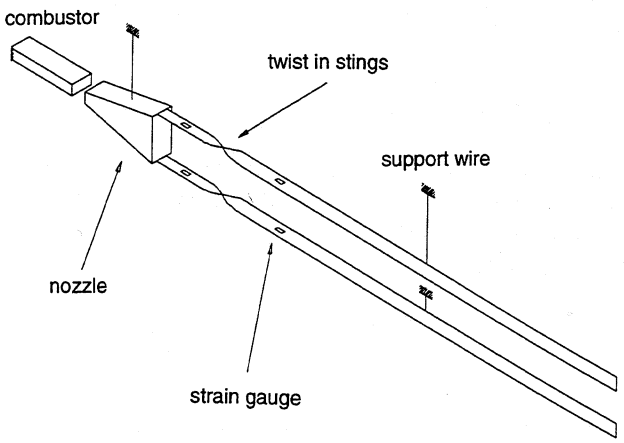

Fig. 4 Schematic of scramjet nozzle on thrust balance.

The nozzle was freely suspended in the T4 shock tunnel behind a fixed scramjet combustor. A Mach 4 contoured nozzle supplied the test gas to the combustor duct. Fuel was injected at the entrance to the combustor duct from a two-dimensional, central, planar strut. The combustor duct was 600 mm long. A lip at the exit of the combustor duct ensured that there was no leakage, while allowing free movement of the nozzle and stings. Around the perimeter of the lip there was approximately 0.5 mm of clearance with the nozzle. This is shown in Fig. 5. The nozzle was shrouded from the external flow and the stings were shrouded from the nozzle flow. Static pressure tappings were located in the ramp walls of the nozzle.

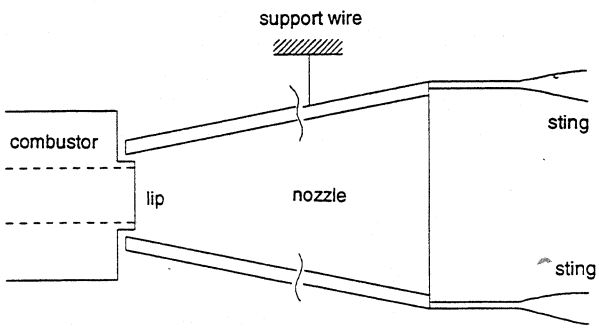

Fig. 5 Details of the lip between the thrust nozzle and combustor.

In Fig. 6 the average of the deconvolved strain measurements from each sting is compared with the thrust calculated from static pressure measurements. The two pairs of curves correspond to fuel-off and fuel-on (combustion) cases at a nozzle supply enthalpy of 9 MJ/kg. The fuel is hydrogen. The difference between the net thrust derived from the strain measurement (solid line) and the pressure thrust (dotted line) is attributed to skin friction and to the small amount of external drag on the nozzle caused by a small amount of flow leaking into the lip region and into the nozzle shielding. The difference between the two pairs of curves for the fuel-off and fuel-on conditions is the increase in thrust due to combustion of the hydrogen.

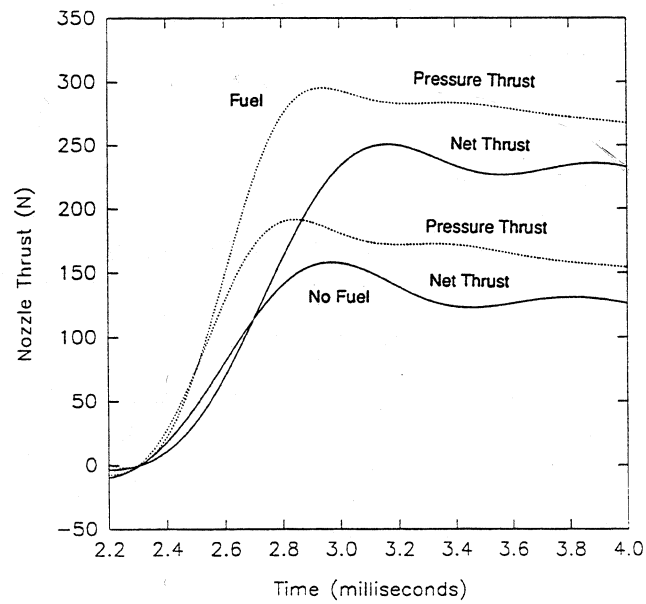

Fig. 6 Deconvolved net thrust and pressure thrust on scramjet nozzle; with and without fuel at 9 MJ/kg supply enthalpy.

The stress wave force balance has also been applied by Stalker et. al. (9) to measurement of the thrust produced by a simple, fully integrated scramjet model, with intakes, combustion chambers, thrust surfaces and exterior surfaces, using a 13% silane 87% hydrogen fuel mixture. These experiments showed that the scramjet model produced net positive thrust at velocities up to 2.4 km/s.

A sketch of the scramjet model and fuel tank is shown in Fig. 7. The scramjet centrebody, shown in streamwise section in the figure, consisted of a conical forebody with 9° half angle, a cylindrical section of 51 mm diameter, and an afterbody of 10° half angle. It was partly surrounded by an axisymmetric cowl which had an internal diameter of 67 mm over the parallel section of the centrebody, and was of 71 mm outside diameter. Filler pieces, which are not shown, divided this parallel section into six constant area combustion chambers, each of which subtended an angle of 26° at the centreline. Fuel was injected through six orifices located at the upstream end of the combustion chambers. The filler pieces between the combustion chambers extended upstream in the form of intake compression ramps which processed the flow in the forebody shock layer through two shocks, each of 8° deflection. The leading edges of the cowl were shaped to prevent these shocks spilling from the intake.

The scramjet model was larger and more complicated than the cones of the previous studies so it was necessary to

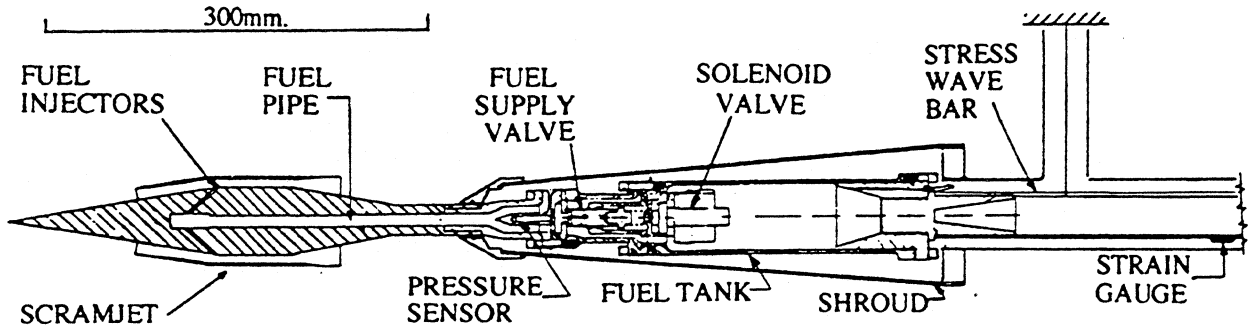

Fig. 7 Scramjet model and fuel tank mounted on balance.

demonstrate by finite element modelling that the impulse response used in the deconvolution process was insensitive to assumptions about the distribution of loading on the model. Fig. 8 displays the results of injecting fuel with air test gas. Prior to the test flow, fuel injection induces a net thrust of 30 N. Then, as the flow over the model is established, the drag increases. However, ignition of the fuel then causes thrust which increases until it becomes quasi-steady at a net thrust of 60 N. This demonstrates that a steady state of thrust can be generated by a scramjet model in the test time of a shock tunnel, and that it can be measured with the stress wave force balance.

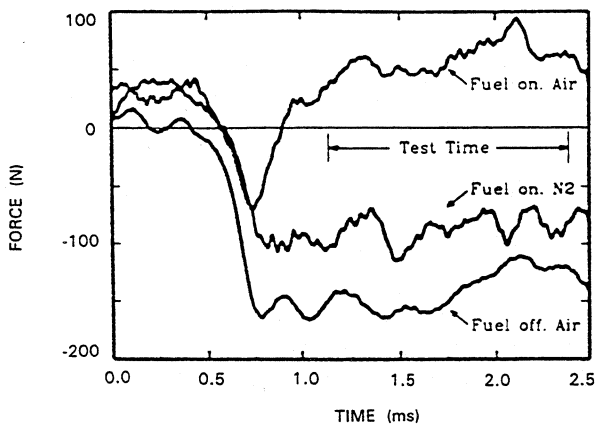

Fig. 8 Time history of net thrust on scramjet when fuel is injected into air and nitrogen test gases and when fuel is not injected and the test gas is air; supply enthalpy 3.2 MJ/kg.

2.4 Forces and Moments on Bodies at Incidence

Use of the stress wave force balance has recently been extended to the measurement of lift, drag and pitching moment on models at incidence to a hypervelocity free-stream. The three-component force balance developed by Mee et. al. (10) is shown attached to a cone at incidence in Fig. 9. It consists of a single, 2 m long sting attached to the test model by four short bars. Each of the bars is instrumented for measurement of axial strain at its mid-point. A strain gauge bridge is also attached to the sting, 200 mm from the model/sting junction. Combinations of the strain signals from the four bars are used to produce two output signals, one responding primarily to a normal force input and the other responding primarily to a pitching moment input. The strain measurement in the sting responds primarily to an axial force input. Inevitably there is some coupling among these output signals.

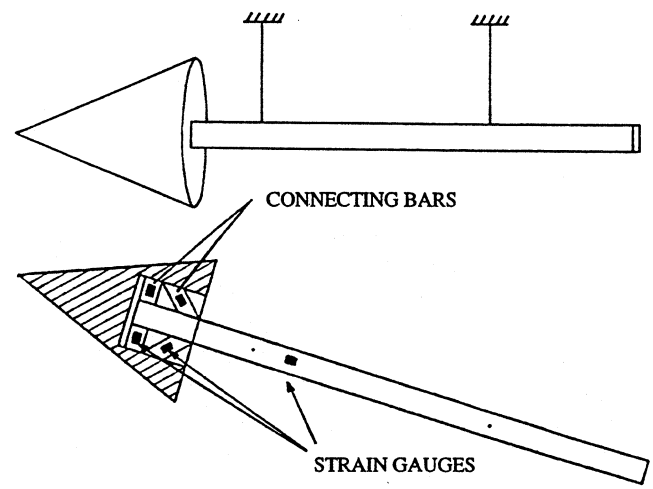

Fig. 9 Schematic of three-component balance attached to cone at incidence.

The time-histories of the three output signals $y_A(t)$, $y_N(t)$ and $y_M(t)$ caused by axial and normal forces and moment, can be related to the time-histories of the axial force, normal force and pitching moment on the model, $u_A(t)$, $u_N(t)$ and $u_M(t)$ via nine impulse response functions. This coupled convolution problem can be written in matrix notation as in (2).

$$\begin{pmatrix} y_A \\ y_N \\ y_M \end{pmatrix} = \begin{pmatrix} G_{AA} & G_{AN} & G_{AM} \\ G_{NA} & G_{NN} & G_{NM} \\ G_{MA} & G_{MN} & G_{MM} \end{pmatrix} \begin{pmatrix} u_A \\ u_N \\ u_M \end{pmatrix} \qquad (2)$$

The y vectors are formed from the discretised output signals and the square G matrices are formed from the impulse response functions, G_{ij} being the impulse response for the y_i output due to a u_i input. The nine impulse response matrices are obtained by a series of bench tests in which a weight is attached to various points on the model by a fine wire and then quickly released. The output signals are processed to produce the impulse responses. The linearity of the system enables the responses to flow-type loading distributions to be

determined by superposition of the results of several tests for single loads applied at various locations on the model.

In experiments in the T4 shock tunnel, each of the y_i outputs is measured and time-domain, coupled deconvolution techniques are used to determine the time-histories of the lift and drag forces and the pitching moment on the model. The prototype three-component balance was installed in a 220 mm long, 15° semi-angle cone as shown in Fig. 9. This configuration was found to be quite insensitive to loading distribution. Experiments were performed to measure the three components of force on the cone for incidences of 0.0°, 2.5° and 5.0°. Sample results are presented in Fig. 10 for a nozzle supply enthalpy of 11 MJ/kg and 5° incidence. The pitching moment is not shown because it is very small.

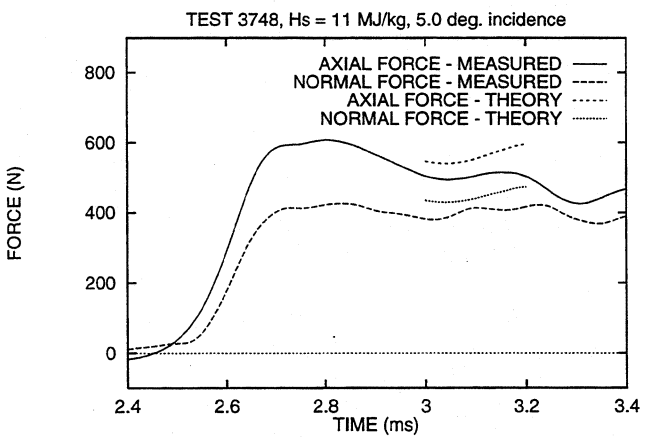

Fig. 10 Time-history of measured and predicted lift and drag on cone at 5° incidence.

The three-component stress wave force balance has also been used to measure the aerodynamic forces on a type of hypersonic vehicle known as a waverider (Anderson et al. (11)). Figure 11 is a schematic of a waverider attached to the rectangular sting of a stress wave force balance. When operating at design conditions the waverider has its bow shock wave on the windward side of the vehicle attached to the leading edges, thus entrapping the high pressure flow so that no leakage occurs to the leeward side. The advantage of this design is that when compared with more conventional designs for hypersonic vehicles, the preserved high pressure will produce a greater lift force for a given angle of attack. This enables the waverider to operate at lower angles of attack where higher lift-to-drag ratios can be obtained. The waverider presently under study at The University of Queensland (Fig. 11) has a theoretical, inviscid lift-to-drag ratio of 2.0. A preliminary result obtained from experiments in T4 is shown in Fig. 12. It indicates a lift-to-drag ratio of about 1.55 in the period of steady test flow which begins at about 1.1 ms in the time-history. This ratio is lower than the theoretical, inviscid result, due to viscous drag effects and the possibility of the test conditions being slightly off-design.

3 PRESSURE MEASUREMENT

Pressure measurement in hypervelocity impulse facilities is

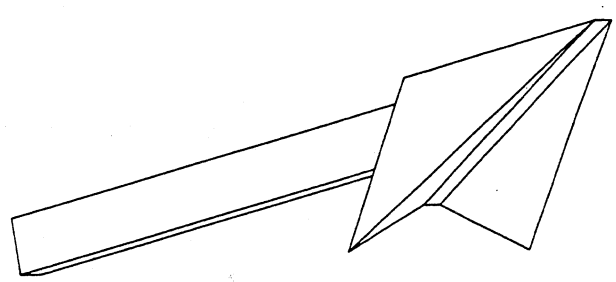

Fig. 11 Schematic of waverider on sting.

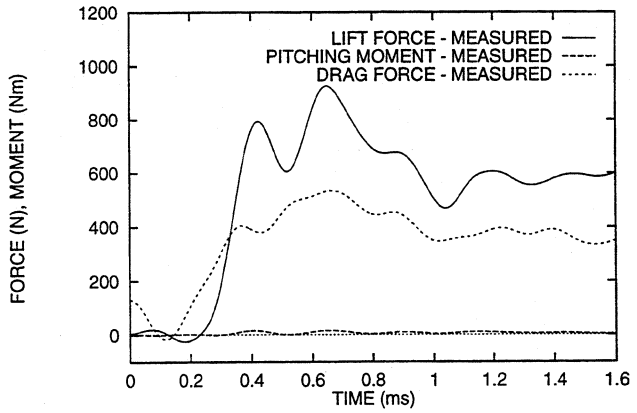

Fig. 12 Measured time-history of lift, drag and moment on waverider; supply enthalpy 8 MJ/kg, Mach 8.

now a standard technique because of the availability of small, fast commercial piezoelectric pressure transducers. In conjunction with the necessary charge amplifiers, such pressure transducers can have rise times of the order of 2 μs. However, to protect their sensitive diaphragms from the impact of small particles in the free-stream and to reduce heating from the flow, they are usually not mounted flush with a model surface. Instead, pressure transducers are mounted in cavities which are connected to the surface by small channels. This mounting configuration increases the rise time of the measurement system but it remains sufficiently short for use in shock tunnels. Due to the very short test times in expansion tubes, protective cavities cannot be employed and the transducer diaphragm must be mounted flush with the surface of the model. This is acceptable, except on windward surfaces inclined significantly to the flow. In these situations diaphragms will be damaged. Then an alternative approach is to use a bar gauge.

The bar gauge shown in Fig. 13 is being developed for measuring Pitot pressure in expansion tubes. The pressure measurement is obtained from the stress waves in the bar. The technique is similar to the principle of the stress wave force balance, except that deconvolution of the output signal is not required because the rise time of the gauge is very short, about 8 μs as shown by the step response in Fig. 14 that was determined from finite element modelling. This short rise time is obtained by matching the mechanical

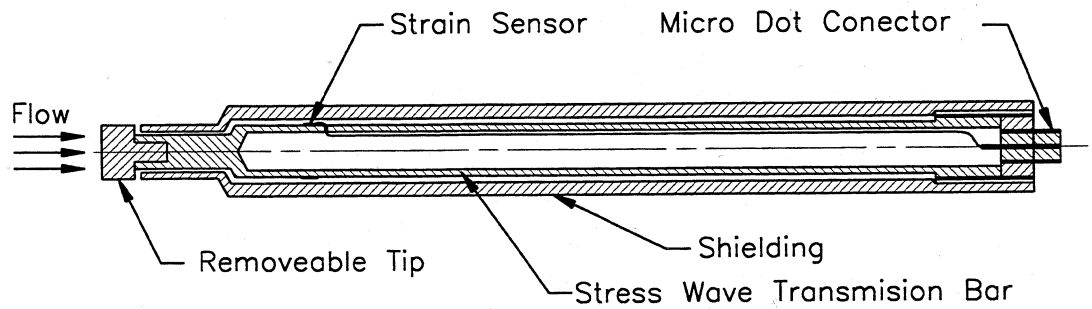

Fig. 13 Schematic of bar gauge.

impedance along the transmission bar. The hollow section enables transition to a larger diameter for ease of application of the strain sensors. The removable tip at the front of the gauge protects the shielding from the impinging flow. Although the tip represents an impedance mismatch with the rest of the bar, the effect is negligible. A correction for nonuniformities in the pressure distribution across the front of the tip can be made through numerical analysis of the flow behind the detached shock wave.

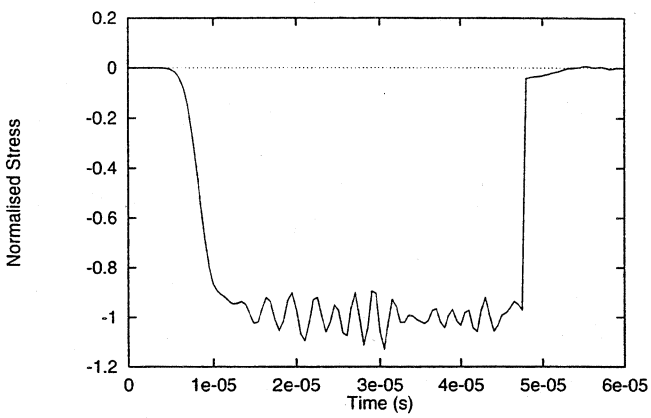

Fig. 14 Computed step response of bar gauge, showing application of load and unloading due to reflection from end of bar.

5 CONCLUSIONS

The principle of the stress wave force balance has been shown to be effective in measuring single- and multi-component forces on a range of models in hypervelocity impulse facilities. In all cases the balances respond within a few hundred microseconds. This is sufficiently fast for use in free-piston shock tunnels and large expansion tubes but further work is needed to adapt the technique to use in smaller expansion tubes where test times are less than 100 μs. This work is in progress, together with extension of the technique to measurement of pressure in expansion tubes.

6 ACKNOWLEDGMENTS

The authors are grateful for the support received from the Australian Research Council under Grant AE9032029 and the Queen Elizabeth II Fellowship Scheme (for D.J. Mee).

7 REFERENCES

1. STALKER, R.J., Development of a Hypervelocity Wind Tunnel, Aero. J., 374-384, June 1972.
2. MILLER, C.G., Operational Experience in the Langley Expansion Tube with Various Test Gases, AIAA J., 12, 195-196, 1978.
3. SIMMONS, J.M., Measurement Techniques in High Enthalpy Hypersonic Facilities, Proc. Third World Conference on Experimental Heat Transfer, Fluid Mechanics and Thermodynamics, Honolulu, Hawaii, 31 Oct.-5 Nov. 1993, 43-60, 1993.
4. SKINNER, K.A., Species Measurements Using Mass Spectrometry in High Mach Number Flows, Proc. of 11th Australasian Fluid Mech. Conf., Univ. of Tasmania, Hobart, Australia, pp. 435-438, Dec. 1992.
5. KELLY, G.M., PAULL, A. and SIMMONS, J.M. Skin friction measurements and Reynolds analogy in a hypersonic boundary layer. 19th International Symposium on Shock Waves, Marseille, France, 1993.
6. SANDERSON, S.R., and SIMMONS, J.M., Drag Balance for Hypervelocity Impulse Facilities, AIAA J., 29, 2185-91, 1991.
7. SIMMONS, J.M., DANIEL, W.J., MEE, D.J. and TUTTLE, S.L. Force Measurement in Hypervelocity Impulse Facilities, New Trends in Instrumentation for Hypersonic Research, A. Boutier (ed.), NATO ASI Series E, Vol. 224, 285-294, Kluwer Academic Publishers, Dordrecht, Netherlands, 1993.
8. TAYLOR, G.I., and MACCOLL, J.W., The Air Pressure on a Cone Moving at High Speed, Proc. Roy.Soc. London, Series A, 139, 278-297, 1932.
9. STALKER, R.J., SIMMONS, J.M., PAULL, A. and MEE, D.J., Measurement of Scramjet Thrust in Shock Tunnels, Paper AIAA 94-2516, 18th AIAA Aerospace Ground Testing Conference, Colorado Springs, CO, 20-23 June 1994.
10. MEE, D.J., DANIEL, W.J., SIMMONS, J.M. and TUTTLE, S.L. Balance for the Measurement of Multiple Components of Force in Flows of a Millisecond Duration. 19th International Symposium on Shock Waves, Marseille, France, 1993.
11. ANDERSON, J.D. Jr., LEWIS, M.J. and KOTHARI, A.P., Hypersonic Waveriders for Planetary Atmospheres, J. Spacecraft, 28, 401-410, 1991.